A Spatial Model for Tumor Drug Resistance: the case of GIST Liver Metastases

Guillaume Lefebvre,Thierry Colin, Olivier Saut, Clair Poignard, Francois Cornelis

May 26, 2014

What is the GIST ?

GIST : Gastro-Intestinal Stromal Tumors

- In 50% of cases, the GIST are metastatic.
- In 50% of metastatic case, metastases are present in the liver.

$\Rightarrow$ 25% of patient with a GIST have a liver metastases.

Current treatment protocol

1. First line: Imatinib, a cytotoxic drug. Inhibits a specific receptor tyrosine kinase (BCR-Abl).

10-15% of patients present a mutation of gene KIT (on exons [4, 5]) that immediately leads to an imatinib insensitivity (see Fig 1b).

For the other patients, the imatinib controls metastatic lesions during a period more or less long: around 20-24 months in 85% of cases (see Fig 1a).

2. Second-line: sunitinib, which is a multi-targeted receptor tyrosine kinase inhibitor (that inhibits PDGFRs, VEGFRs and KIT), which has both cytotoxic and antiangiogenic effects.

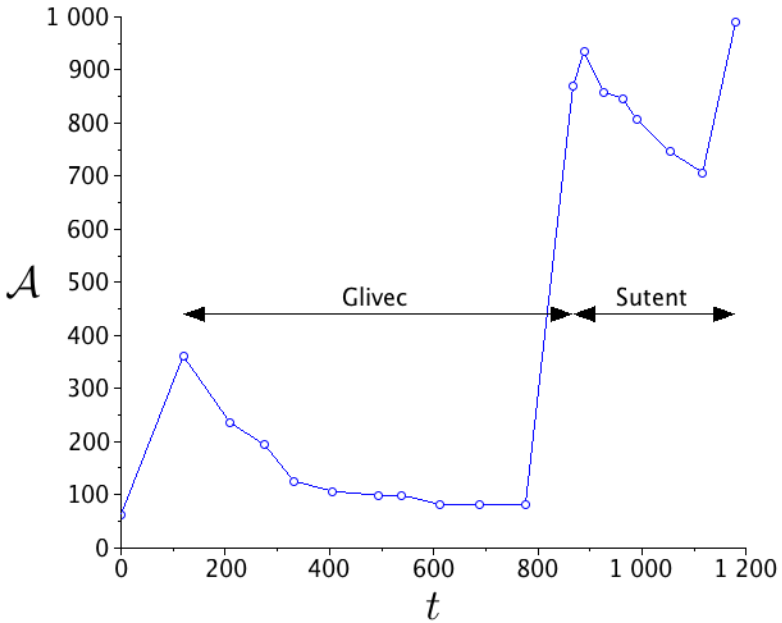

(A) Patient A: profile that has a good answer on treatment – x-axis: time in days; y-axis: the tumor area in mm^2.

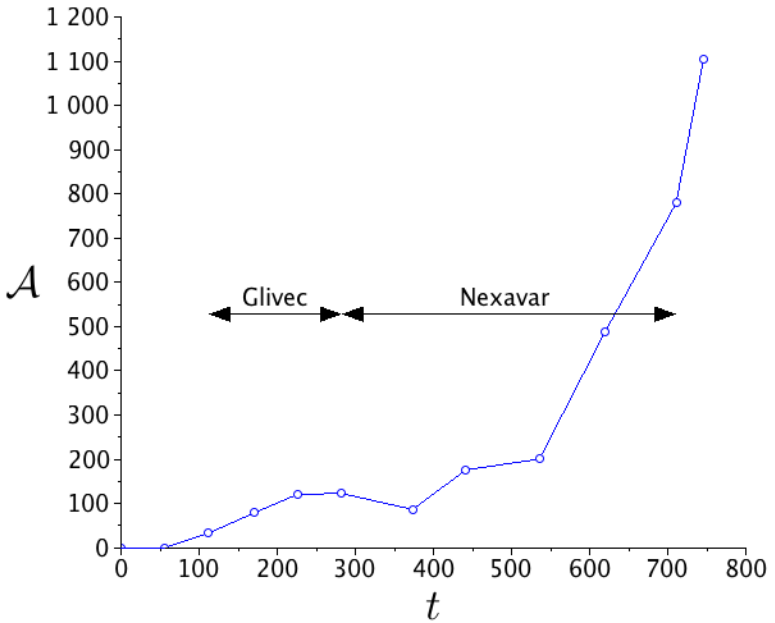

(B) Patient E: typical profile of resistance to Imatinib associated to a particular genetic mutation (EXON11) – x-axis: time in days; y-axis: the tumor area in mm^2.

FIGURE: Evolution of a GIST for two differents patients: one representing the most common case and the other one a patient with a mutation

Therapeutic follow-ups of patient

CT-scans (usually every 2 months)
$\rightsquigarrow$ Track the disease evolution and the response to the treatment.

Clinicians challenge: optimizing cancer treatments and particularly the switch time from the first-line to the second-line treatment, in order to increase the overall survival time.

RECIST criteria: the diameter of the largest lesions is the *only* information extracted from the CT-scan.

Our aim

Develop a mathematical model based on medical images of liver metastases of locally advanced GIST in order to determine, for *each* patient:

- the treatment response
- the relapse times after the first-line and the second-line treatments
- geometric specificities of tumor growth

Our model enable to:

- Compare the model with the medical images
- Highlight more crucial data such as tumor heterogeneities and geometrical properties of the tumor growth, which may provide more precise indicators than the RECIST criteria.

The existing models

Several theoretical tumor growth models have been developed:

- ODEs model as Mendelsohn, logistic, Gompertz or Bertalanffy ([9] and in [– ref Papier Seb –]) $\rightsquigarrow$ This kind of models fit data only on the tumor volume
- Cellular automata [1, 8]
- Models based on mixture theory [2]
- Agent-based models [10]
- Models based on fluid mechanics [7]
- Models based on reaction-diffusion theory [11]

$\Rightarrow$ Several scale, from the cells to the tissues, are covered by this large variety of models.

Our choice: a model based on fluid mechanics.

Contents

CT-scans I

Cross-section selected is the same for all exams.

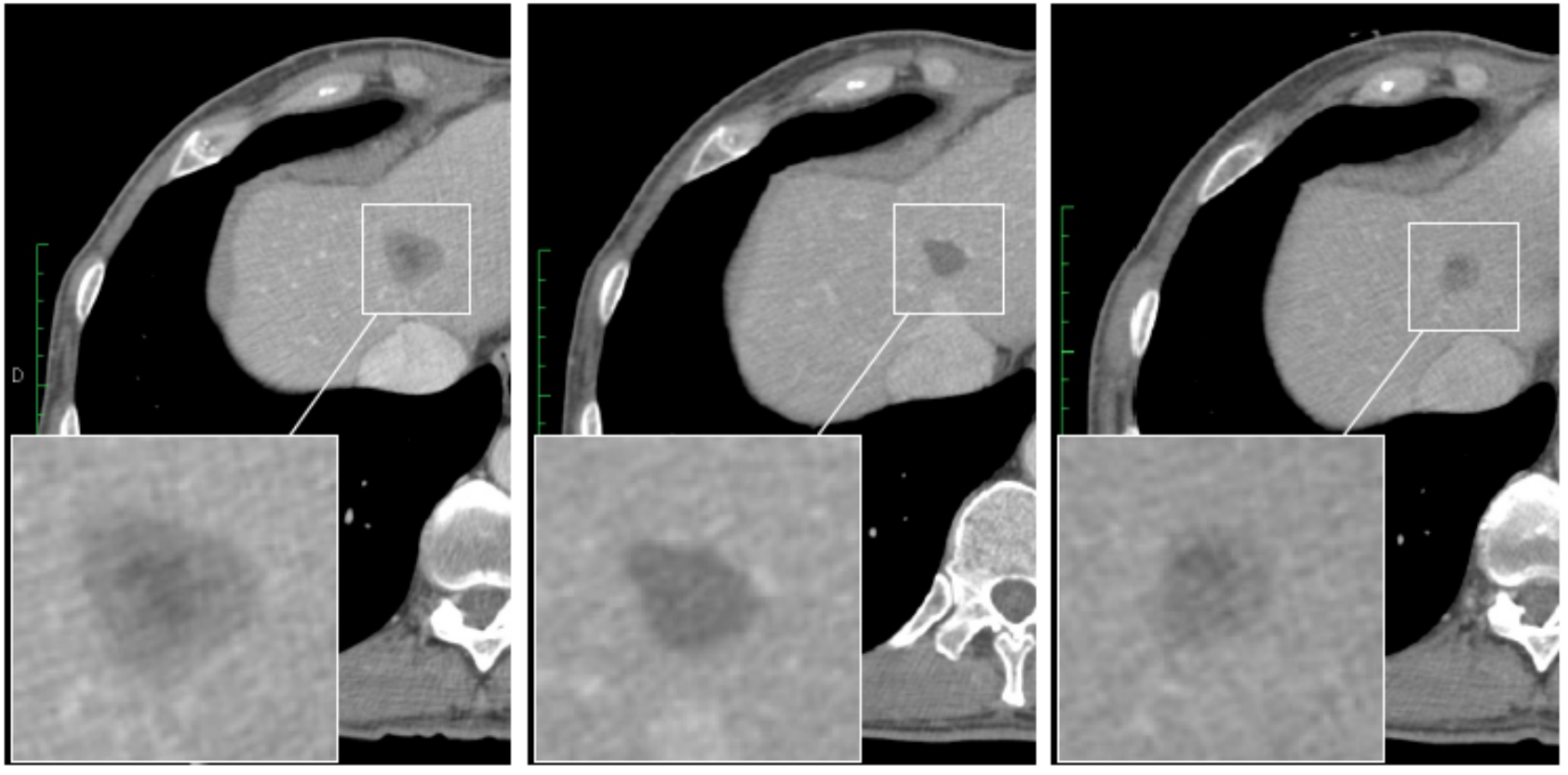

(A) Sept 16, 2008 – Day 119 (B) June 30, 2009 – Day 406 (C) July 5, 2010 – Day 776

CT-scans II

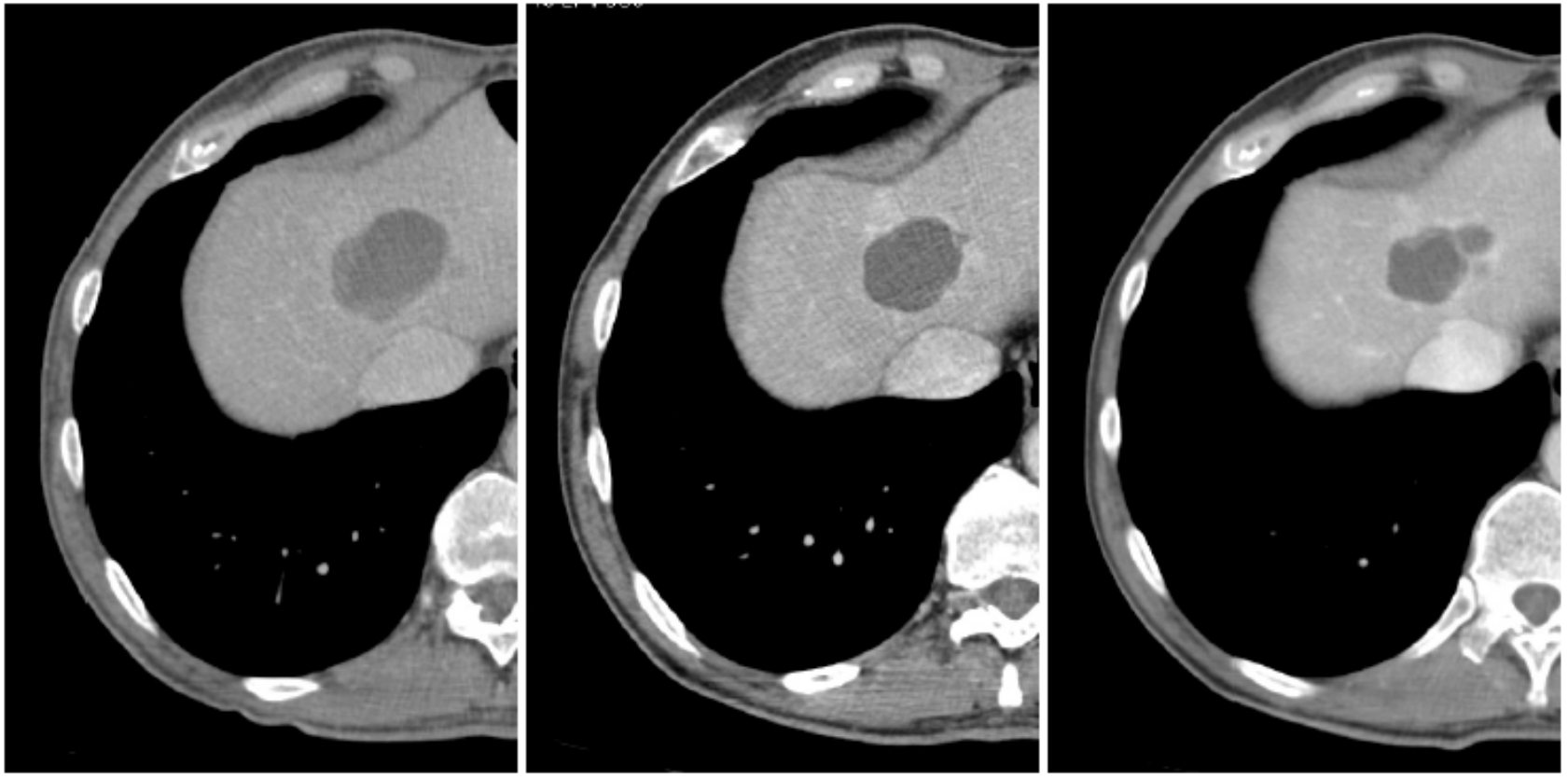

(D) Oct 25, 2010 – Day 888 (E) Jan 7, 2011 – Day 962 (F) June 10, 2011 – Day 1116

FIGURE: Spatial evolution of the patient A metastasis on a series of CT-scans

GIST are characterized by the presence of some *heterogeneity* in the tumor.
The following facts are visible on the CT-scans :

1. During the initial growth, the tumor is very heterogeneous
2. During the first phase of the evolution with the Glivec (cytotoxic drug), the lesion becomes smaller and very homogeneous: this may correspond to a low cellular activity
3. Just before the relapse, some heterogeneity appears: a rim of proliferative cells is visible while the center is composed of necrotic cells (darker) Let us note that even if the cellular division has started again, the tumor area has not yet increase.
4. When the Glivec failure is obvious (increase of area), clinicians switch treatment. Here, an antiangiogenic treatment is tried: the Sutent.

5. From D) to E), the tumor area decreases again. The tumor darkens: this may correspond to an increase of necrotic cells rate in a tumor. The heterogeneity is also reduced. However, the phenomenon is less important than under Glivec.
6. Before the new therapeutic failure, the tumor is very heterogeneous again.

$\Rightarrow$ RECIST criteria is *not* a good criteria to evaluate the response to antiangiogenic drug

Evolution of the mass of the tumor

Brightness of voxels

↕

Density of the tissue

↕

Level of necrosis

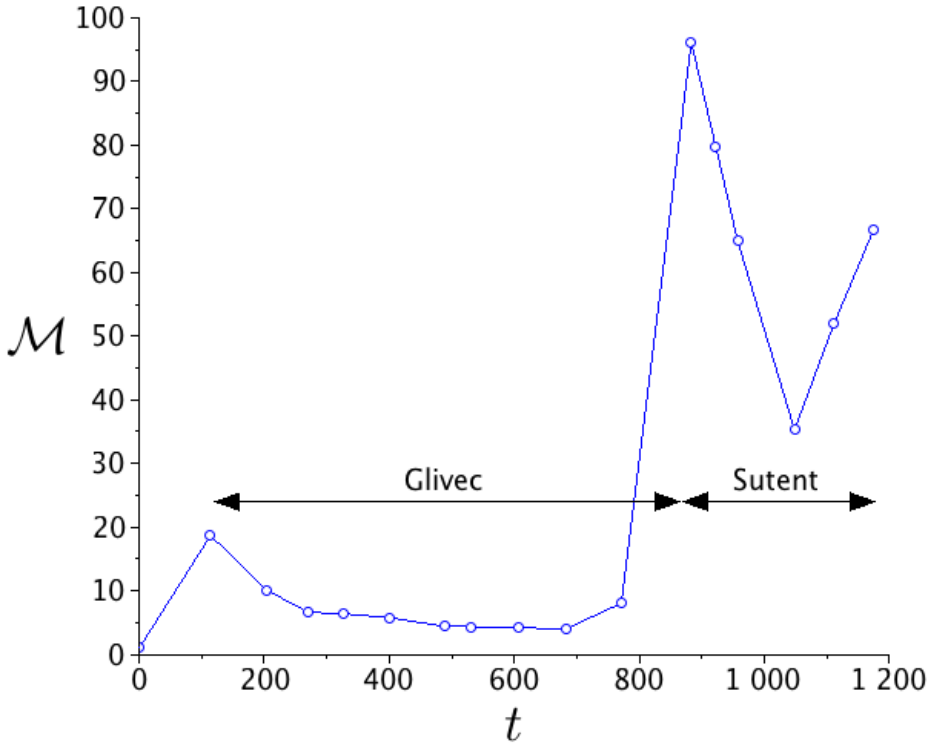

Figure: Patient A: tumor mass evolution (normalization of integral of grey levels) as a fonction of time in days.

Main hypothesis I

- Cells are represented by severall populations and we compute the density of the population [6].
  No strong biological evidence of this hypothesis.
  $\rightsquigarrow$ Probably, mutated cells do not exist from the beginning but appear during the evolution. The mutation can occur
  - before the liver invasion
  - just after the colonization when the metastasis is still too small to be visible on CT-scan
- Angiogenesis plays a crucial role in tumor growth $\Rightarrow$ we will need to introduce a model to describe it [3]:
  - The growth of P-cells (proliferatives cells) will be controlled by the quantity of oxygen.
  - This oxygen is transported through the bloodstream.
  - This bloodstream grows according to a concentration gradient of VEGF (Vascular Endothelial Growth Factor)
  - VEGF is itself controlled by the P-cells and hypoxia.

Main hypothesis II

Here, crude model of angiogenesis (to keep the model as simple as posssible) [12]:
$\rightsquigarrow$ We consider direct impact of the P-cells on the speed of migration of oxygen

- Spatial expansion of the tumor is governed by a collective velocity induced by the growth of the volume (only a passive movement, no active invasion process is taken into account).
  N.B: This assumption would not be correct for a primary tumor.

List of variables

Name	Meaning	Unit
$P_1(t, \mathbf{x})$	Fraction of cells that are both sensitive to imatinib (Glivec) and sunitinib (Sutent)	-
$P_2(t, \mathbf{x})$	Fraction of cells that are resistant to imatinib and sensitive to sunitinib	-
$P_3(t, \mathbf{x})$	Fraction of cells that are both resistant to imatinib and sunitinib	-
$N(t, \mathbf{x})$	Fraction of necrotic cells	-
$S(t, \mathbf{x})$	Fraction of healthy cells	-
$M(t, \mathbf{x})$	Fraction of oxygen // Vascularization	-
$\xi(t)$	Average velocity of oxygen transport in direction of the tumor	$cm.d^{-1}$
$\mathbf{v}(t, \mathbf{x})$	Velocity of the passive movement of the tumor under the pressure	$cm.d^{-1}$
$\Pi(t, \mathbf{x})$	Medium pressure	$kg.cm^{-1}.d^{-2}$

Table: List of variables – $d = \text{day}$

List of parameters I

Name	Meaning	Unit	Value for fit patient A	Value for fit patient B
γ_0	Tumor cells growth rate	d^{-1}	2.0e-2	6.33e-3
γ_1	Tumor cells apoptosis rate	d^{-1}	8.0e-3	4.46e-2
C_S	Health tissue apoptosis rate compared to γ_1	-	10	10
M_{th}	Hypoxia threshold	-	2	2
μ	Elimination rate of the necrotic tissue by the imune system	d^{-1}	1.33e-2	8.19e-2
ψ	Diffusion rate of the oxygen	$cm^2.d^{-1}$	1.33e-2	3.33e-3
η	Consumption rate of tumor cells	d^{-1}	6.67e-2	8.05e-3
α	Angiogenic excitability	d^{-1}	1.11e-3	8.0e-3
λ	Elimination rate of angiogenic growth factor signal	d^{-1}	2.0e-2	0.68
C_0	Angiogenic capacity of health tissue	d^{-1}	3.33e-2	3.33e-2
k	Tissue permeability	$kg^{-1}.cm^$	1	1

List of parameters II

Name	Meaning	Unit	Value for fit patient A	Value for fit patient B
δ	Patient sensitivity to imatinib and imatinib dosage	d^{-1}	7.17e-3	3.45e-3
C_g	Sunitinib dose efficiency	-	0.8	0.90
ν	Cytotoxic effects of the sunitinib	d^{-1}	5.33e-3	3.33e-4
ϵ_{th}	Minimal proportion of tumor cells in a tissue that can be detected on scans – Treshold that delimite the tumor area	-	1.0e-2	0.1
Σ_{ini}	$(P_2 + P_3)_{t=0}$	-	3e-06	0.10
q_{ini}	$(P_3/P_2)_{t=0}$	-	7.5e-3	0.41
ξ_{ini}	Growth factor signal at time $t = 0$	$cm.d^{-1}$	3.33e-3	0

Table: List of parameters – $d = \text{day}$

Growth rate

R : Numerical parameter – commands the regularisation of the Heaviside step function.

$$\gamma_{pp}(M) = \frac{\gamma_0}{2}\Big(1 + \tanh\big(R(M - M_{th})\big)\Big) \quad (2.1)$$

$$\gamma_{pd}(M) = \frac{\gamma_1}{2}\Big(1 - \tanh\big(R(M - M_{th})\big)\Big) \quad (2.2)$$

$$\gamma_{sd}(M) = C_S\gamma_1 \max\Big(0, -\tanh\big(R(M - M_{th})\big)\Big) \quad (2.3)$$

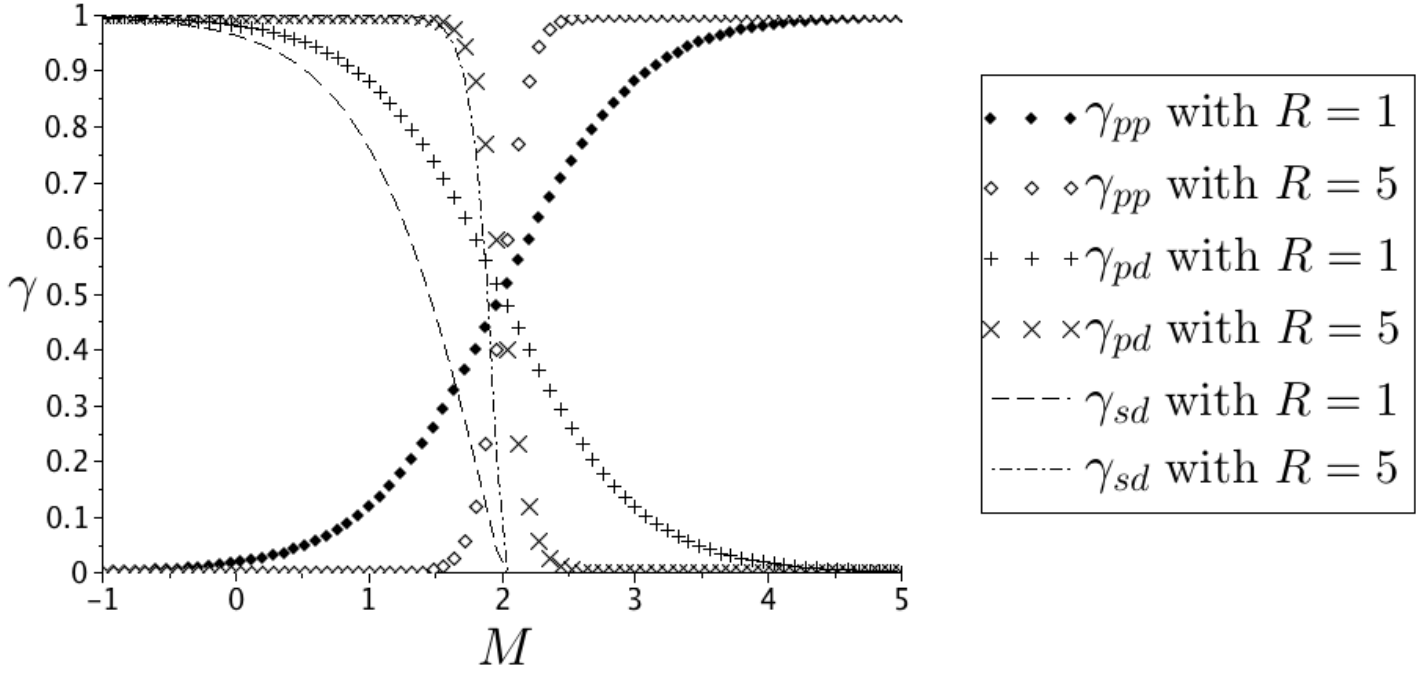

PDEs on populations

$$\partial_t P_1 + \nabla.(vP_1) = (\gamma_{pp} - \gamma_{pd})P_1 - f(t)(1+M)P_1 - \nu(1-g(t))(1+M)P_1 \quad (2.4)$$

$$\partial_t P_2 + \nabla.(vP_2) = (\gamma_{pp} - \gamma_{pd})P_2 - \nu(1-g(t))(1+M)P_2 \quad (2.5)$$

$$\partial_t P_3 + \nabla.(vP_3) = (\gamma_{pp} - \gamma_{pd})P_3 \quad (2.6)$$

$$\partial_t N + \nabla.(vN) = \gamma_{pd}(P_1+P_2+P_3) + \gamma_{sd}S - \mu(1+M)N + f(t)(1+M)P_1 + \nu(1-g(t))(1+M)(P_1+P_2) \quad (2.7)$$

— Elimination of necrosis
— Action of Glivec $f(t)$
— Cytotoxic action of Sutent $g(t)$

We assume that :

$$\partial_t S + \nabla.(vS) = -\gamma_{sd}S \quad (2.8)$$

By denoting $P = \sum_i P_i$ and by adding above equations, we obtain:

$$\nabla.v = \gamma_{pp}P - \mu(1+M)N \quad (2.9)$$

Angiogenesis

$$\partial_t \xi_1 = \alpha \int_\Omega \left(1.1 - \frac{\gamma_{pp}}{\gamma_0}\right)(P_1 + P_2) g \, \mathrm{d}x - \lambda \xi_1 \quad (2.10)$$

$$\partial_t \xi_2 = \alpha \int_\Omega \left(1.1 - \frac{\gamma_{pp}}{\gamma_0}\right) P_3 \, \mathrm{d}x - \lambda \xi_2 \quad (2.11)$$

By considering the sum, we have :

$$\partial_t \xi = \alpha \int_\Omega \left(1.1 - \frac{\gamma_{pp}}{\gamma_0}\right)\left[(P_1 + P_2) g + P_3\right] \mathrm{d}x - \lambda \xi \quad (2.12)$$

- $\xi_1(t)$: Average concentration of VEGF.
- $\xi_2(t)$: Average concentration of others growth factors.
- λ : Elimination rate of angiogenic signal.
- α : Production rate of angiogenic signal.

Vascularization

$$\partial_t M - \xi \frac{\nabla S}{\|\nabla S\|} \nabla M = \underbrace{C_0 S \left(1 - \frac{M}{2M_s}\right)}_{\substack{\text{We impose} \\ M = 2M_s \text{ in} \\ \text{health tissue.}}} \overbrace{- \eta P M}^{\substack{\text{Destruction of} \\ \text{blood network caused} \\ \text{by tumor growth.}}} + \psi \Delta M$$

- η : Destruction rate of blood network.
- ψ : Rate of diffusion.

Notice that :

- More the angiogenic signal is important, more the vascularization is transported.
- The vascularization is transported from the health tissue to the tumor.

System closure

$\Pi(t,x)$: Pressure

$v(t,x)$: Global speed of cells induced by the pressure.

$k(t,x)$: Tissue permeability

Darcy's law :

$$v = -k\nabla\Pi \tag{2.13}$$

where :

$$k(t,x) = k_0 S + k_1 P + k_2 N \tag{2.14}$$

Numerically: $k = 1$

A reasonable variation of k not influenced the numericals results.

Mesh and Method

- 2D cartesian staggered grid $\Omega = [0, L] \times [0, D]$
- Finite volume method
- Fraction of cells are discretized in the center of cells and the velocities are discretized on a middle of each edge of cells

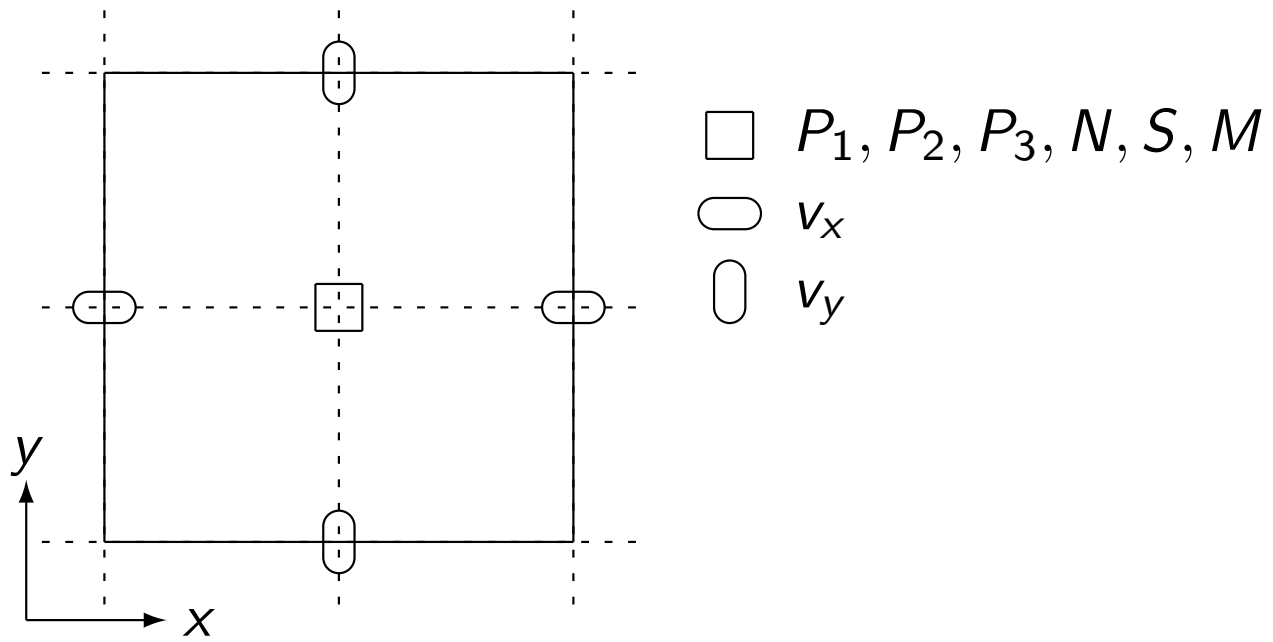

Figure: Discretization of unknown variables on typical cell.

Pressure and velocity calculation

1. Initial data : P_1, P_2, P_3, N, S and M at the initial time $t = 0$
2. Δt computating with respect the CFL.
3. Pressure computing. By (2.9) and (2.13), we obtain:

$$\begin{cases} -\nabla.(k\nabla\Pi) = F & \text{on } \Omega, \\ \Pi = 0 & \text{on } \partial\Omega, \end{cases} \tag{3.1}$$

   where $F = \gamma_{pp}P - \mu(1+M)N$.
   $\longrightarrow$ Classical 5-points scheme.
4. Velocity field computing, (thanks to Darcy's law (2.13))
5. Cell populations advection.

Advection equation

Thanks to $P + N + S = 1$, we can compute S from P and N. Numerically, we compute only the following set of 4 equations:

$$\begin{cases} \partial_t W + \nabla.(\mathbf{v}W) = G(W, M) & \text{on } \Omega, \\ W = 0 & \text{on } \partial\Omega, \end{cases} \tag{3.2}$$

where $W = {}^t(P_1, P_2, P_3, N)$, and the function G is defined by the relation (2.4) - (2.6) and (2.7). We solve these equations with a splitting time method:

$$\partial_t W + \mathbf{v}\nabla W = 0 \qquad \text{then} \tag{3.3}$$

$$\partial_t W = G - WF. \tag{3.4}$$

Non-conservative transport
$\Rightarrow$ No guarantees that $0 \leq W_i \leq 1$, for $i = 1, \ldots, 4$.
$\Rightarrow$ High order method (WENO5) in order to minimize this violation.
The equation (3.4) is solved by an Euler or RK3 method.

Vascularization computation

6. $\xi(t)$: Euler or RK3 method to solve the growth factor signal scalar, Eq (2.12).
7. $M(t,x)$:(5) is splitted as follows:

$$\partial_t M - \psi \Delta M = \xi \frac{\nabla S}{\|\nabla S\|} \nabla M \qquad \text{then} \qquad (3.5)$$

$$\partial_t M = C_0 S \left(1 - \frac{M}{2M_{th}}\right) - \eta P M. \qquad (3.6)$$

- Eq. (3.6) is solved by an Euler or RK3 method
- Eq. the equation on vascularization (3.5) is computed as a heat diffusion equation in which the second member is the WENO5 flow.

We impose a Dirichlet condition on the boundary for M:

$$M = 2M_{th} \quad \text{on } \partial\Omega. \qquad (3.7)$$

CFL condition

- CFL condition for WENO5 (including the transport of M):

$$\Delta t \leq \min\left(\frac{\Delta x}{\max|v_x|}, \frac{\Delta y}{\max|v_y|}, \frac{\min(\Delta x, \Delta y)}{\max \xi}\right). \tag{3.8}$$

- CFL due to the splitting method:

$$\Delta t \leq \min_{i=1,\ldots,4}\left(\frac{1}{\max|G_{i,A} - F|}\right). \tag{3.9}$$

(where $G_{i,A}$ is the linear part of the second member of the advection equations) and (for the vascularization):

$$\Delta t \leq \min\left(\frac{1}{\eta}, \frac{1}{\lambda}\right). \tag{3.10}$$

- Arbitrary limit:

$$\Delta t \leq 30 \min(\Delta x, \Delta y). \tag{3.11}$$

Quantities of interest

ϵ_{th}: the minimal fraction of tumor cells in a tissue that can be detected on scans.
With this threshold, we can introduce some quantities as tumor area and mass or the sames for each populations cells:

$$\mathcal{A} := \int \mathbb{1}_{\{P+N>\epsilon_{th}\}}(\mathbf{x})\,\mathrm{d}\mathbf{x}. \tag{3.12}$$

$$\mathcal{A}_J := \int \mathbb{1}_{\{J>\epsilon_{th}\}}(\mathbf{x})\,\mathrm{d}\mathbf{x}, \quad J \in \{P_1, P_2, P_3, N\}. \tag{3.13}$$

$$\mathcal{M}_J := \int J\,\mathrm{d}\mathbf{x}, \quad J \in \{P_1, P_2, P_3, N\}, \tag{3.14}$$

$$\mathcal{M} := \int P\,\mathrm{d}\mathbf{x}. \tag{3.15}$$

CT-scan view reconstitution

Aim: compare the numericals simulations with the CT-scans
$\Rightarrow$ We need to reconstruct a CT-scan view from the quantities of our model: P, N and S.
$\rightarrow$ Interpolation of grey level to get a sort of Hounsfield unit (HU) scale.
$\rightarrow$ Interpolation coefficient are experimentaly fixed ($\tau_P = 0.65, \tau_N = 0.15$ and $\tau_S = 0.8$) thanks to the CT-scan.

We can plotting our numericals results in a grey level by:

$$\tau_P P + \tau_N N + \tau_S S \tag{3.16}$$

Consistency of the model

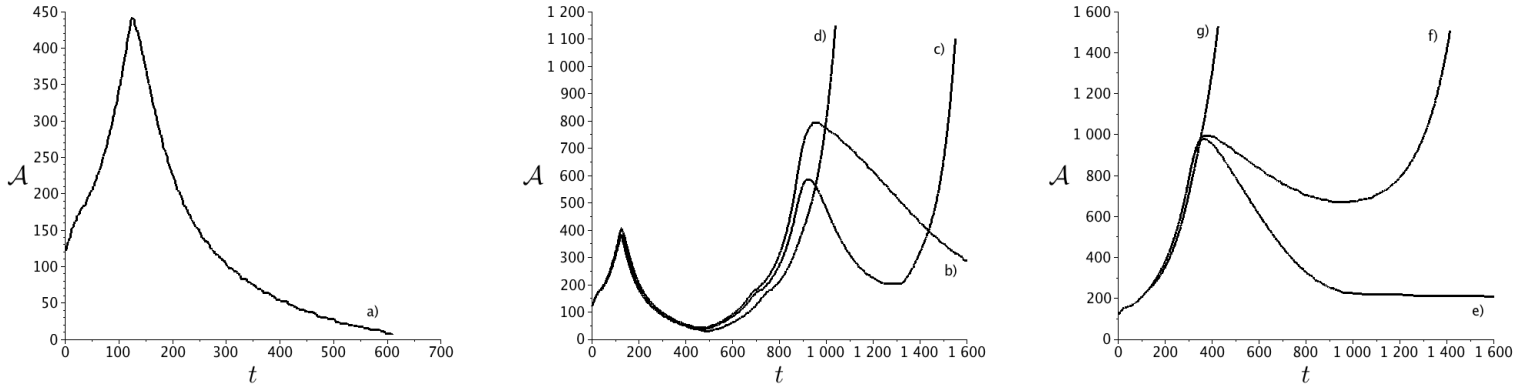

(A) Glivec from 119^{th} day

(B) Glivec from 119^{th} day until 867^{th} day and Sutent just after

(C) Glivec from 119^{th} day until 300^{th} day and Sutent just after

Figure: Several behaviors that the model is able to reproduce

++ : A large range of behavior is take into account.

– – : The model is not be predictive.

Patient A

120 points in each direction // CFL: 0.4.

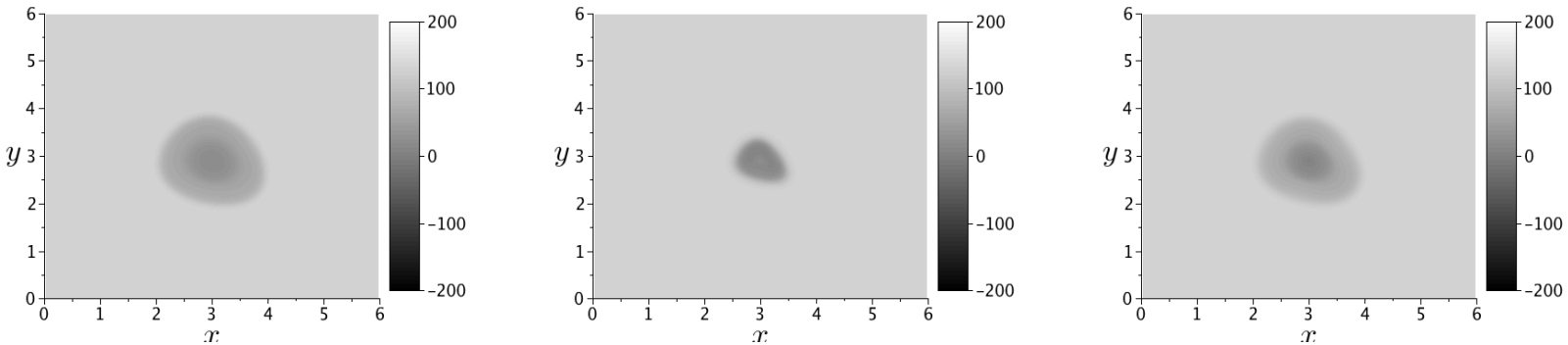

(A) Day 119 (B) Day 409 (C) Day 778

(D) Day 870 (E) Day 961 (F) Day 1120

Figure: Numerical simulations for patient A: spatial evolution of the lesion with CT-scans reconstitution view.

Scan - Patient A (1) Scan - Patient A (2)

Patient A

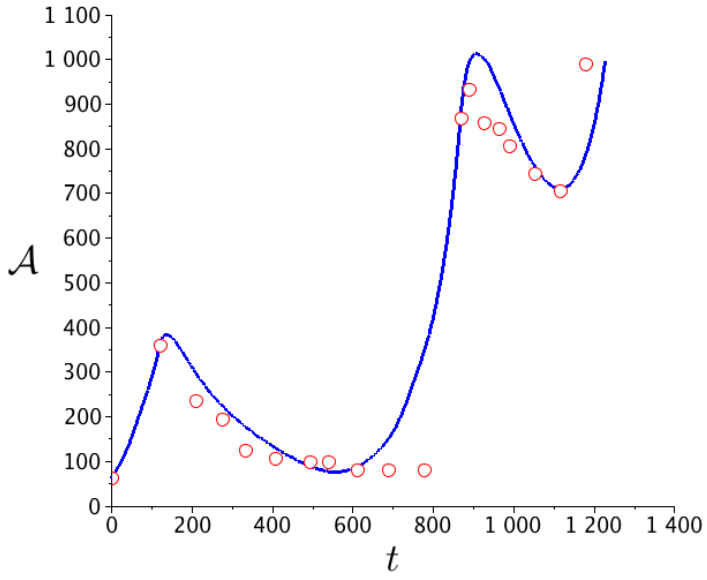

Figure: Numerical fit of the tumor area (Patient A)

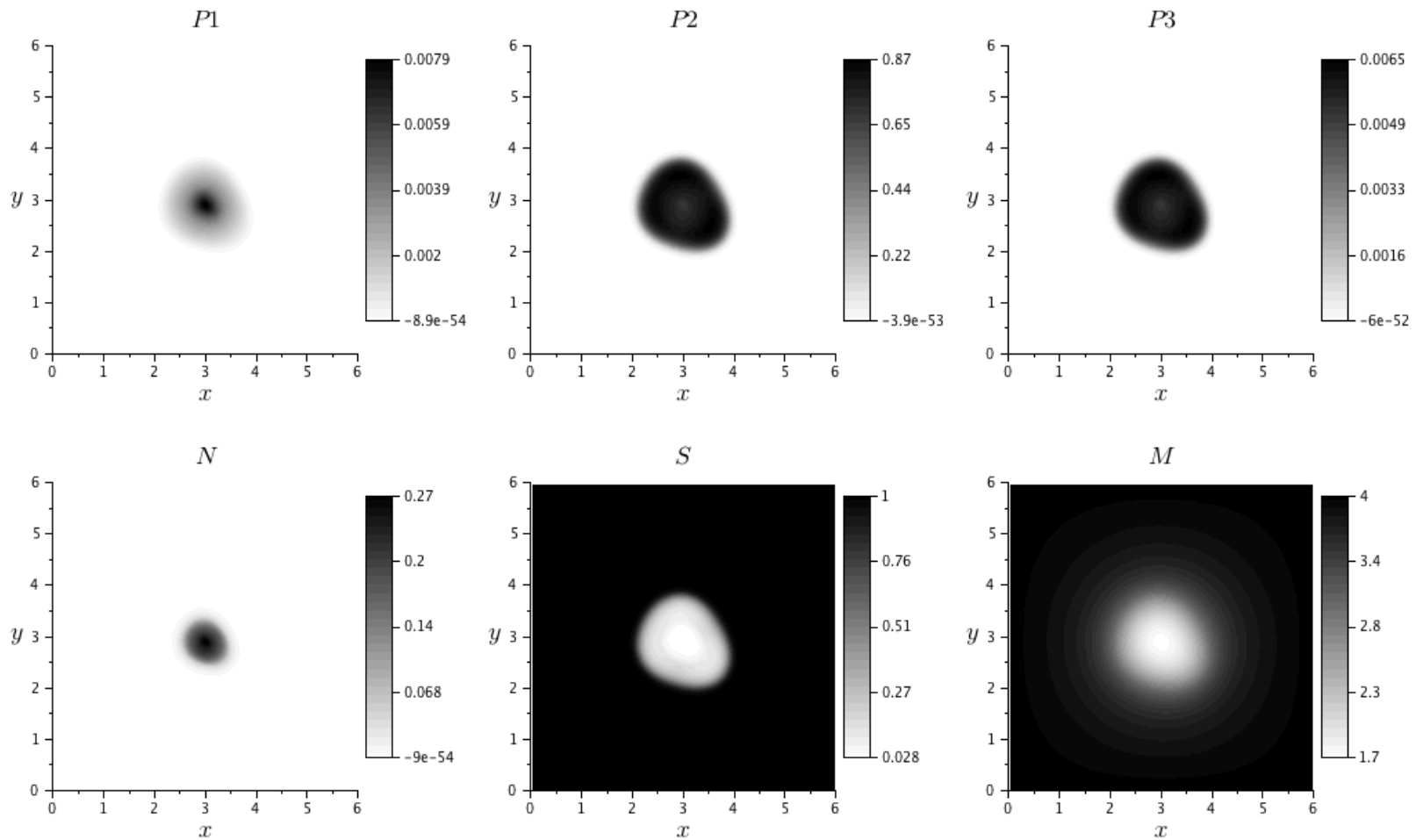

(A) Day 778

FIGURE: Population repartition of patient A given by the numerical simulation. The unit of x-axis and y-axis are cm and the grey level represents the fraction of these populations.

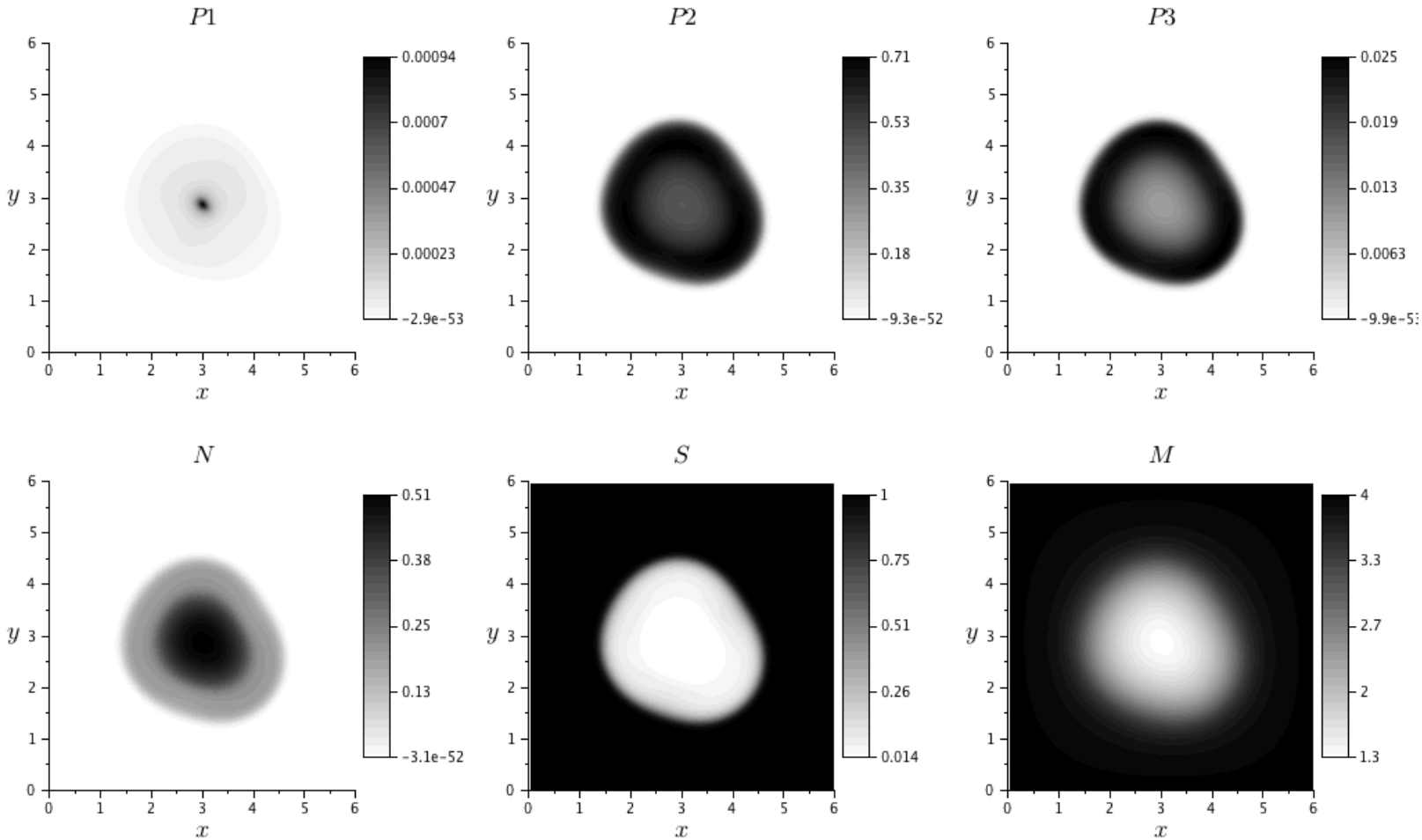

(B) Day 961

FIGURE: Population repartition of patient A given by the numerical simulation. The unit of x-axis and y-axis are cm and the grey level represents the fraction of these populations.

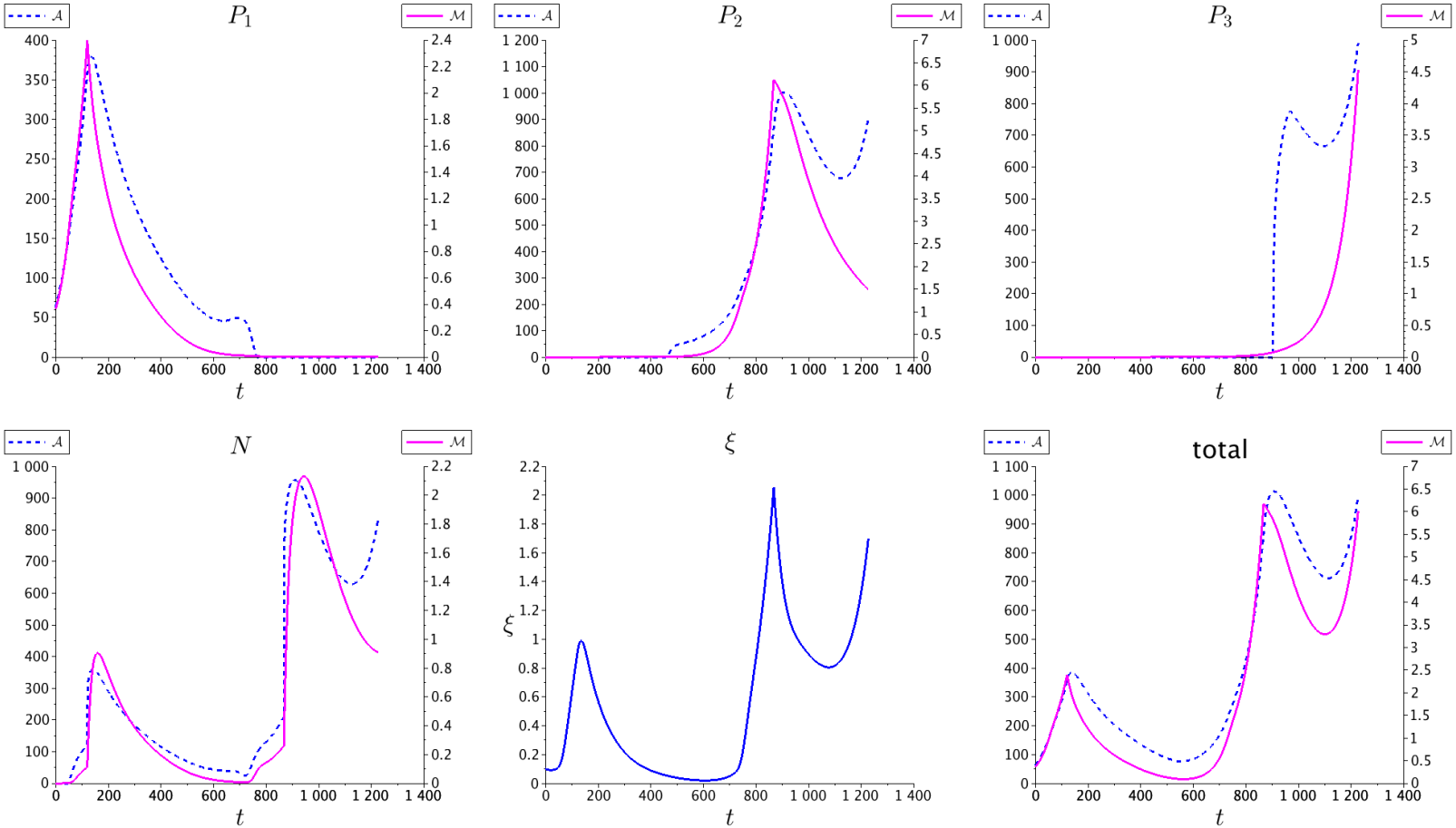

FIGURE: Evolution of the mass (arbitrary unit) and the area (mm^2) of each cellular population and angiogenic signal evolution ($cm.d^{-1}$) given by the numerical simulation.

Patient B I

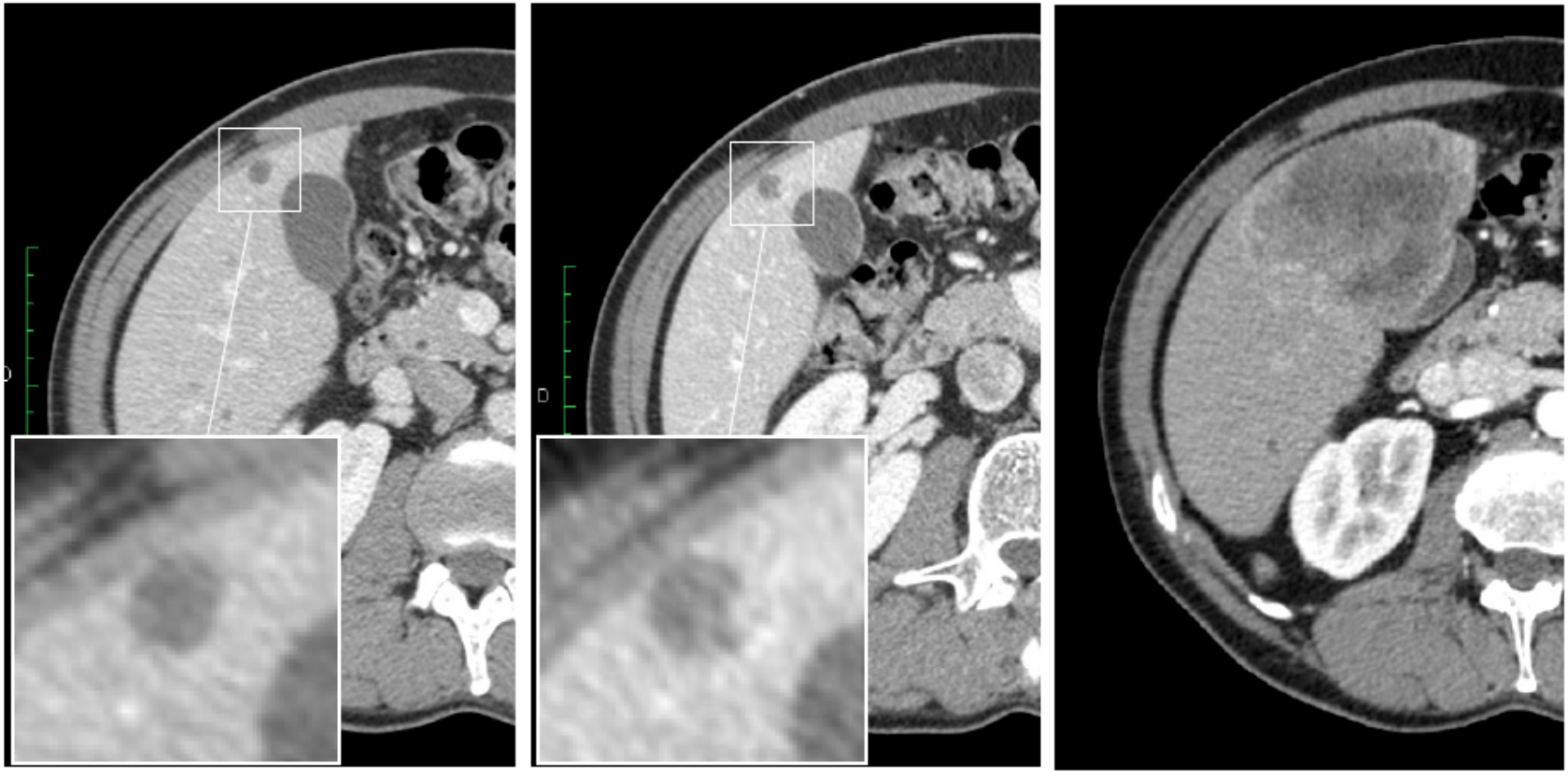

(A) May 23, 2007 – Day 0 (B) July 25, 2008 – Day 429 (C) Sept 14, 2009 – Day 845

Patient B II

(d) April 06, 2010 – Day 1049 (e) Sept 28, 2010 – Day 1224 (f) May 20, 2011 – Day 1458

Figure: Spatial evolution of the patient B metastasis on a series of CT-scans.

As the patient studied in previous section, we try to numerically reproduce the behavior of this tumor with our model.

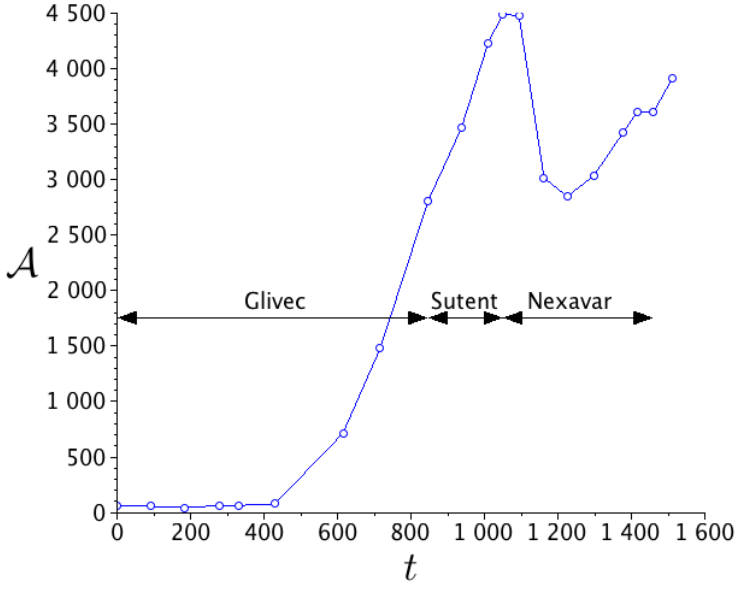

FIGURE: Patient B: evolution (in days) of the tumor area (in mm^2) measured on MRIs

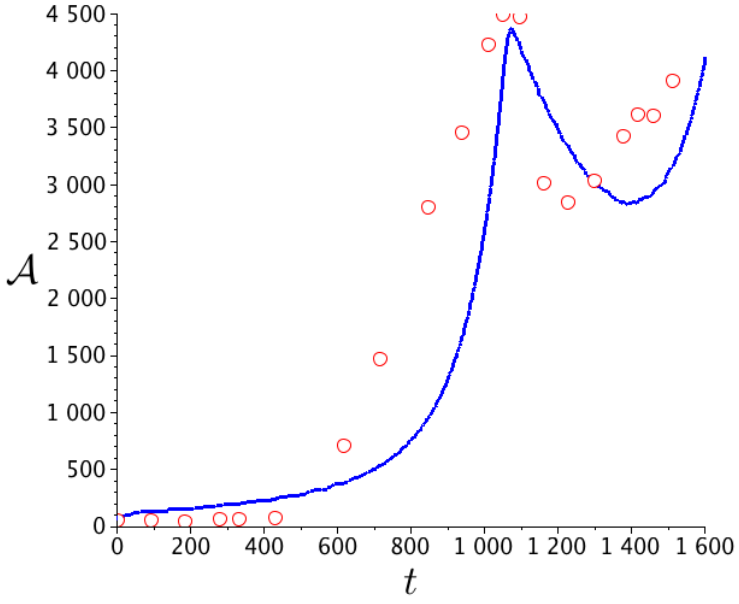

FIGURE: Numerical fit of the tumor area (on patient B) with a priori set of parameters.

Good result but ...

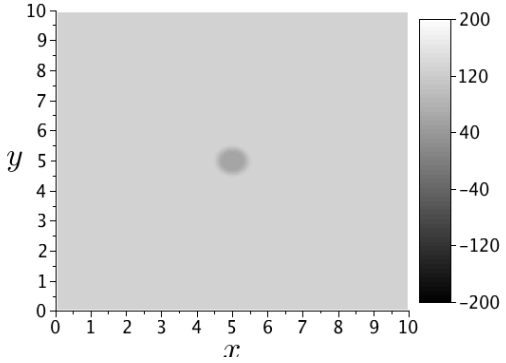

(A) Day 0

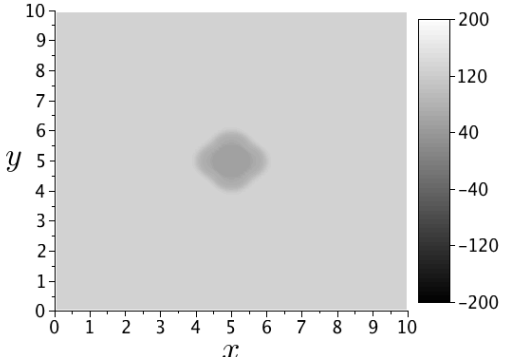

(B) Day 543

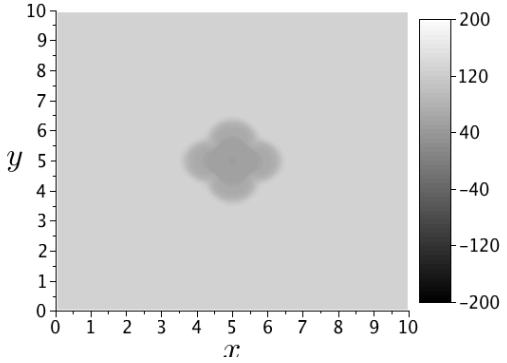

(C) Day 724

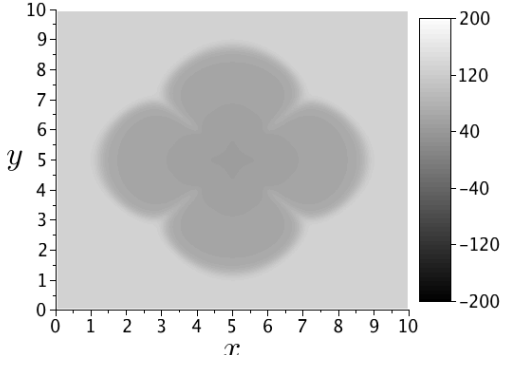

(D) Day 1053

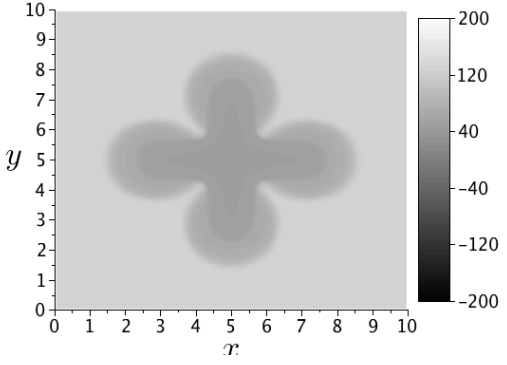

(E) Day 1399

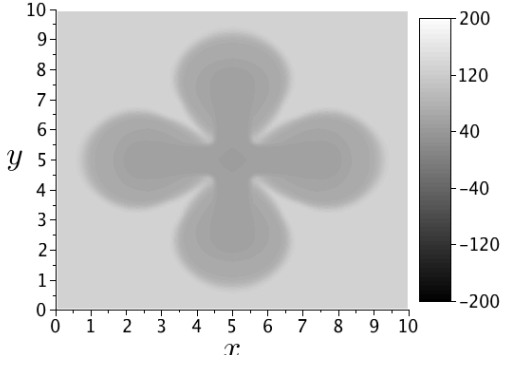

(F) Day 1600

FIGURE: Numerical simulations a priori for patient B: spatial evolution of the lesion with CT-scans reconstitution view. The units of x-axis and y-axis are *cm* and the unit of grey scale is arbitrary.

Adaptation of WENO5 scheme: twin-WENO5

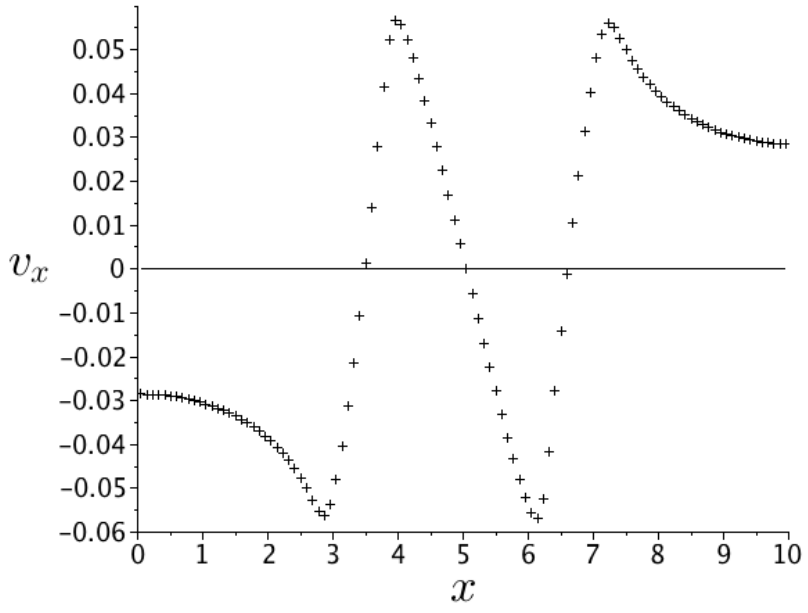

Figure: Cut of velocity (in $mm.d^{-1}$) on $y = 6\ cm$ on 1103^{th} day in function of abscisse x (in cm).

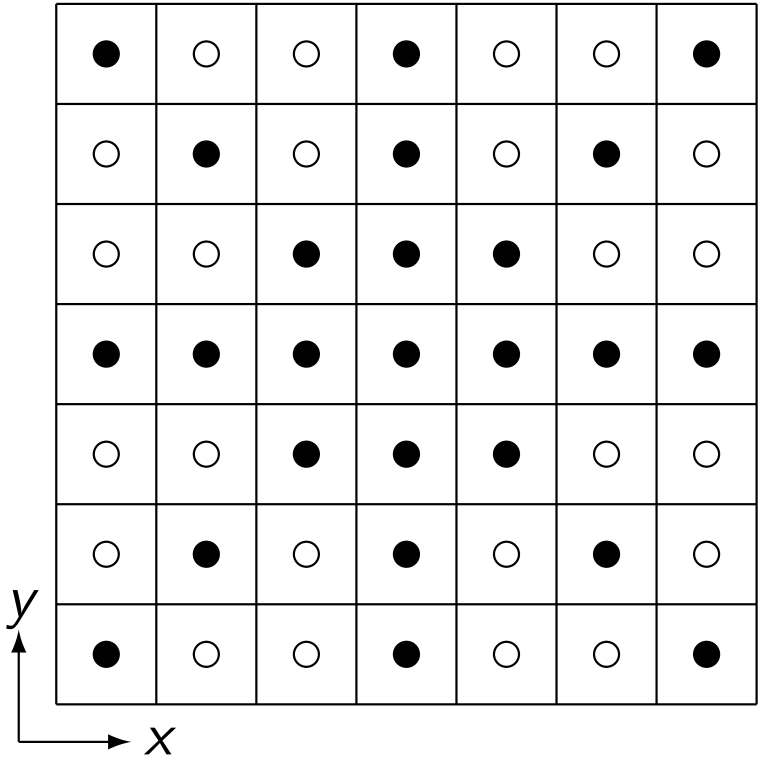

Figure: Stencil of the twin-WENO5 scheme.

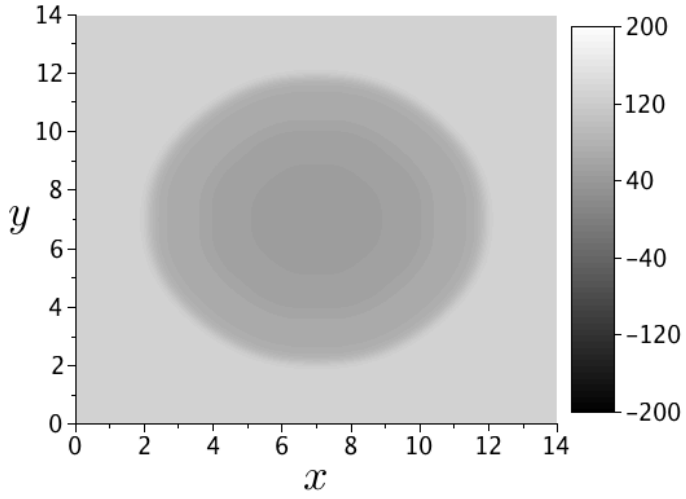

(A) Spatial aspect of the tumor with CT-scan view reconstitution on day 1366. The units of x-axis and y-axis are cm for and the unit of grey scale is arbitrary.

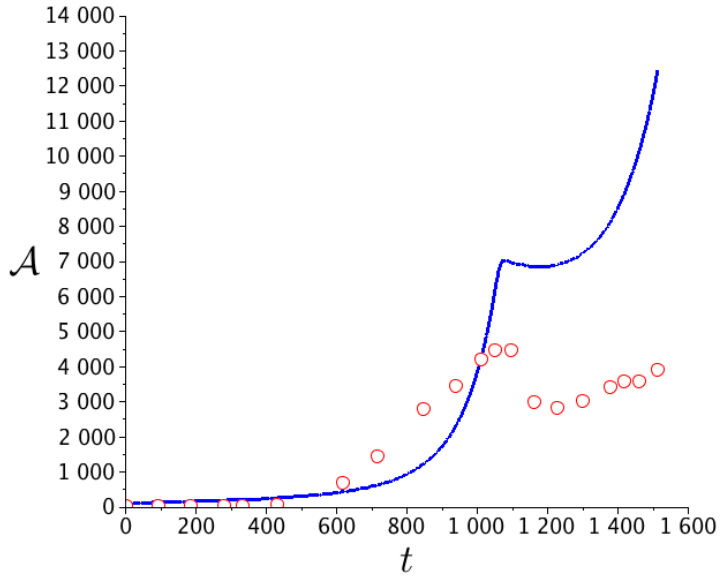

(B) Evolution (in days) of tumor area (in mm^2).

FIGURE: Numerical simulation with first correction with twin-WENO5 scheme ($\beta = 0.26$).

Patient B: Simulation with twin-WENO5

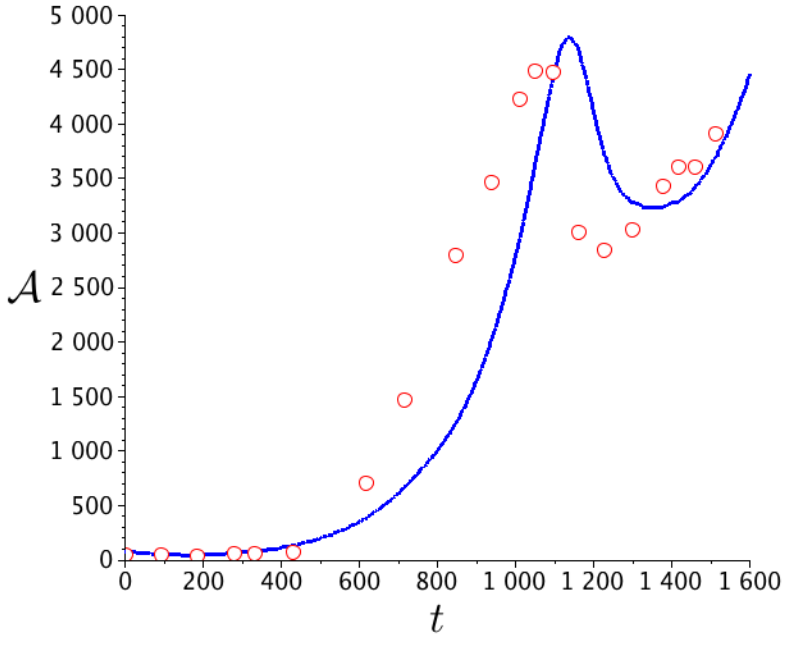

Figure: Evolution (in days) of the tumor area (in mm^2) given by the model for patient B.

Patient B: Simulation with twin-WENO5

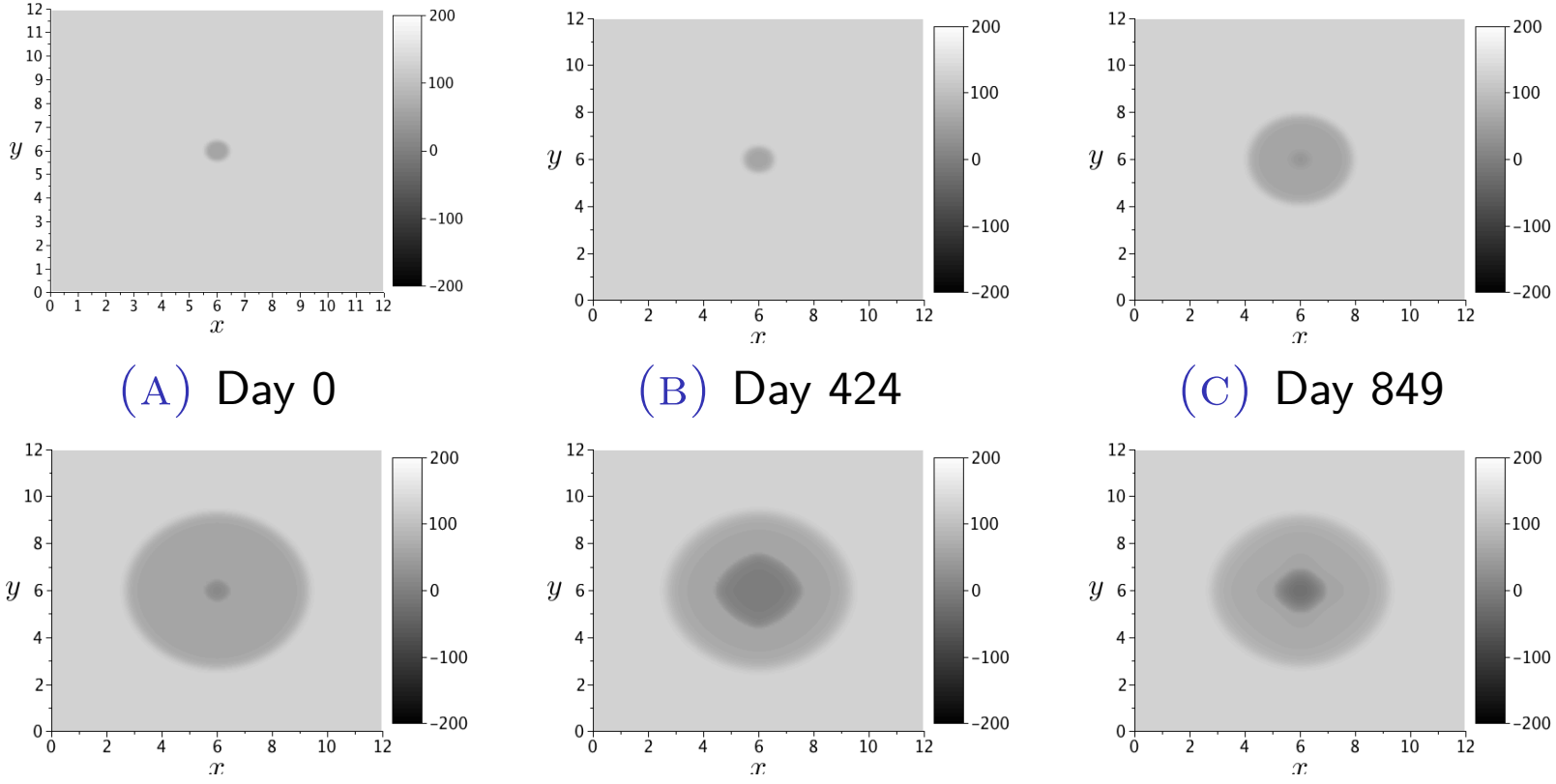

(A) Day 0 (B) Day 424 (C) Day 849

(D) Day 1052 (E) Day 1222 (F) Day 1460

Figure: Numerical simulations with twin-WENO5 ($\beta = 0.3$) for patient B: spatial evolution of the lesion with CT-scans reconstitution view. The units of x-axis and y-axis are *cm* and the unit of grey scale is arbitrary.

Conclusion

- Our model is able to reproduce the global behavior of metastasis during the several stage.
- We can mimic both the control of tumor area by the drugs and the relapse.
- Our results are in agreement with the CT-scans.
- We highlight the heterogeneity levels that may be observed in a metastasis. The more the metastases are heterogeneous, the more the relapse is rapidely occurring.This result reinforces the fact that the RECIST criteria is not sufficient to evaluate the efficiency of a treatment.
- Our model is in according with the pharmocological studies on treatment (minimum threshold to have an action, and existence of an optimum dose)

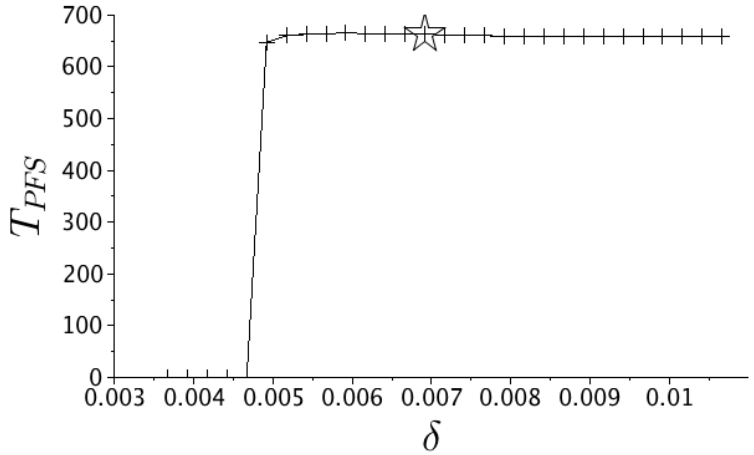

(A) Progression free survival time (T_{PFS} in days) in function of the dose δ

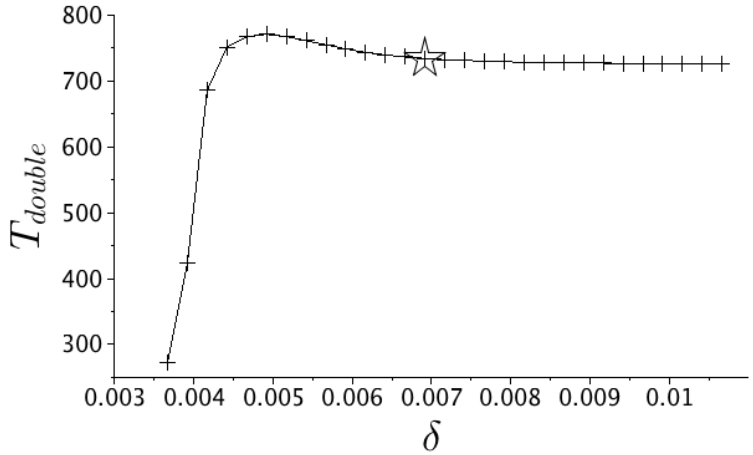

(B) Time corresponding to the growth of tumor area by a factor 2 (T_{double} in days) in function of the dose δ

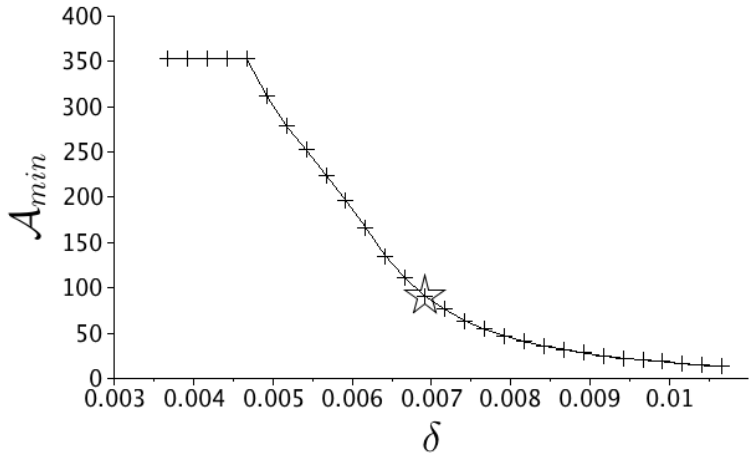

(C) Minimal area reached ($\mathcal{A}_{min}$ in mm^2) in function of the dose δ

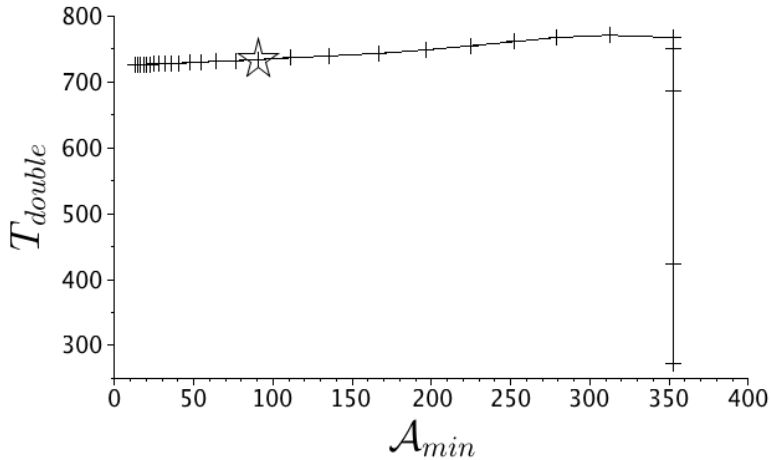

(D) Phase portrait

FIGURE: Glivec efficiency on patient A

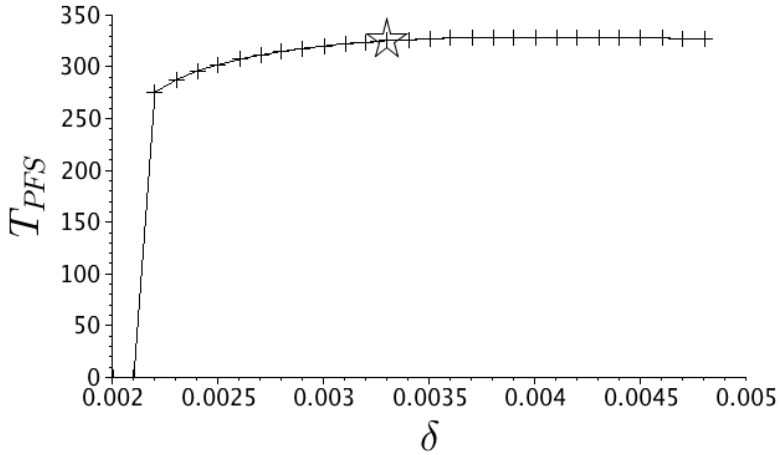

(A) Progression free survival time (T_{PFS} in days) in function of the dose δ

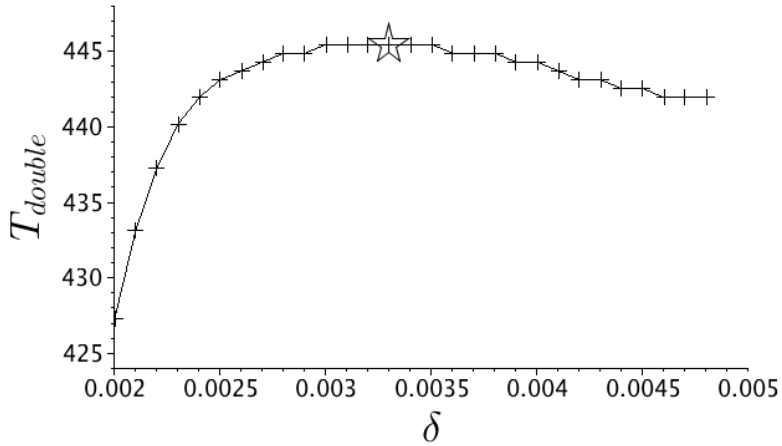

(B) Time corresponding to the growth of tumor area by a factor 2 (T_{double} in days) in function of the dose δ

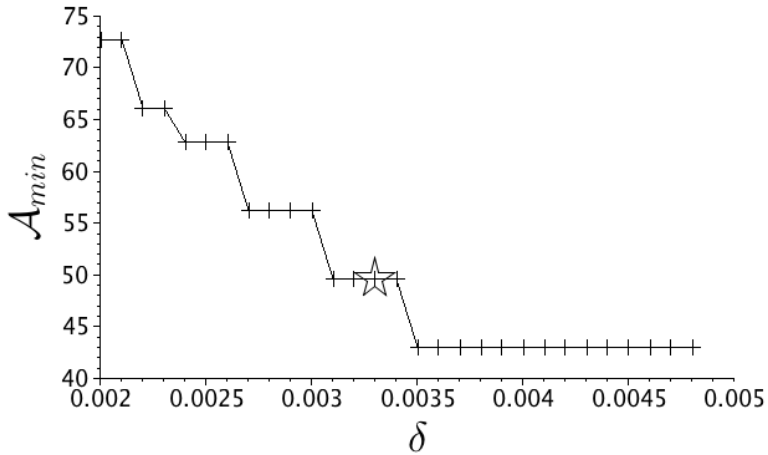

(C) Minimal area reached ($\mathcal{A}_{min}$ in mm^2) in function of the dose δ

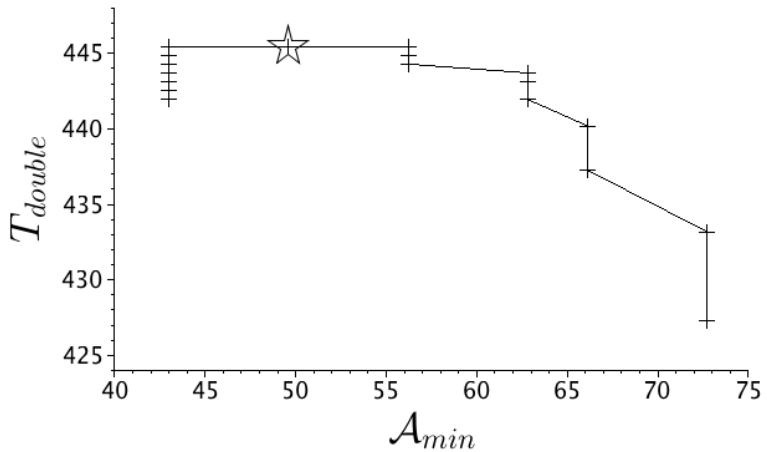

(D) Phase portrait

FIGURE: Glivec efficiency on patient B

That's all

Thanks for your attention.

References I


T. Alarcn, H.M. Byrne, and P.K. Maini.
A cellular automaton model for tumour growth in inhomogeneous environment.
Journal of Theoretical Biology, 225(2):257 – 274, 2003.


D. Ambrosi and L. Preziosi.
On the closure of mass balance models for tumor growth.
Mathematical Models and Methods in Applied Sciences, 12(05):737–754, 2002.


Frédérique Billy, Benjamin Ribba, Olivier Saut, Hélène Morre-Trouilhet, Thierry Colin, Didier Bresch, Jean-Pierre Boissel, Emmanuel Grenier, and Jean-Pierre Flandrois.
A pharmacologically based multiscale mathematical model of angiogenesis and its use in investigating the efficacy of a new cancer treatment strategy.

References II

Journal of Theoretical Biology, 260(4):545 – 562, 2009.

Jean-Yves Blay.
A decade of tyrosine kinase inhibitor therapy: Historical and current perspectives on targeted therapy for GIST.
Cancer Treatment Reviews, 37(5):373 – 384, 2011.

JY Blay, A Le Cesne, PA Cassier, and IL Ray-Coquard.
Gastrointestinal stromal tumors (GIST): a rare entity, a tumor model for personalized therapy, and yet ten different molecular subtypes.
Discov Med, 13(72):357–67, May 2012.

References III

Didier Bresch, Thierry Colin, Emmanuel Grenier, Benjamin Ribba, and Olivier Saut.
A viscoelastic model for avascular tumor growth.
Discrete And Continuous Dynamical Systems, Volume 2009:101–108, 2009.

Thierry Colin, Angello Iollo, Damiano Lombardi, and Olivier Saut.
System identification in tumor growth modeling using semi-empirical eigenfunctions.
Mathematical Models and Methods in Applied Sciences, 22(06):1250003, 2012.

References IV


D Drasdo and S Höhme.
Individual-based approaches to birth and death in avascular tumors.
Mathematical and Computer Modelling, 37(11):1163 – 1175, 2003.
Modeling and Simulation of Tumor Development, Treatment, and Control.


P. Gerlee.
The model muddle: in search of tumor growth laws.
Cancer research, 73(8):2407–11, 2013.

References V


Yuri Mansury, Mark Kimura, Jose Lobo, and Thomas S. Deisboeck.
Emerging patterns in tumor systems: Simulating the dynamics of multicellular clusters with an agent-based spatial agglomeration model.
Journal of Theoretical Biology, 219(3):343 – 370, 2002.


R. Rockne, Jr. Alvord, E.C., J.K. Rockhill, and K.R. Swanson.
A mathematical model for brain tumor response to radiation therapy.
Journal of Mathematical Biology, 58(4-5):561–578, 2009.

References VI

Olivier Saut, Jean-Baptiste Lagaert, Thierry Colin, and Hassan M. Fathallah-Shaykh.
A multilayer grow-or-go model for GBM: Effects of invasive cells and anti-angiogenesis on growth.
Preprint submitted, 2013.